

UCLA

UCLA Previously Published Works

Title

Sub-Nano Clusters: The Last Frontier of Inorganic Chemistry

Permalink

<https://escholarship.org/uc/item/08h872nm>

Authors

Alexandrova, Anastassia N
Bouchard, Louis-s

Publication Date

2014-10-20

DOI

10.1002/9781118949702.ch3

Peer reviewed

Sub-nano clusters: the last frontier of inorganic chemistry

Anastassia N. Alexandrova* and Louis-S. Bouchard

Department of Chemistry and Biochemistry, University of California, Los Angeles, Los Angeles, California, 90095-1569. California NanoSystems Institute, 570 Westwood Plaza, Building 114, Los Angeles, CA 90095.

* Corresponding Author's e-mail: ana@chem.ucla.edu

Abstract: Small inorganic clusters formed by just a few atoms of either main group elements, or transition metals are mysterious species that exhibit a wealth of chemical bonding phenomena, way beyond what established chemistry has to offer. The article overviews the recent developments in the theory of chemical bonding of clusters, and demonstrates how cluster-based technology could benefit from it.

Keywords: clusters, chemical bonding, cluster design, cluster materials, catalysis

1. Introduction

Sub-nano inorganic clusters formed by just a few atoms of either main group elements, or transition metals are mysterious species. It might be appealing to view them as miniature nanoparticles or tiny chunks of the bulk solid, but beware: they have nothing in common with the structure of the extended solid or even of larger nanoparticles. Sub-nano clusters often have unusual structures that do not obey our intuition, such as those shown in Figure 1 (Alexandrova et al. 2012; Cui et al. ; Galeev et al. 2012; Zhai et al. 2003; Zubarev and Boldyrev 2009). In their electronic structure, clusters are most reminiscent of molecules. However, for molecules the rules of chemical bonding are well

developed, and they are instrumental in predicting and rationalizing their structures and properties, whereas for clusters these rules have until just recently not existed at all. The recent developments in the theory of chemical bonding of clusters are the central subject of the present article.

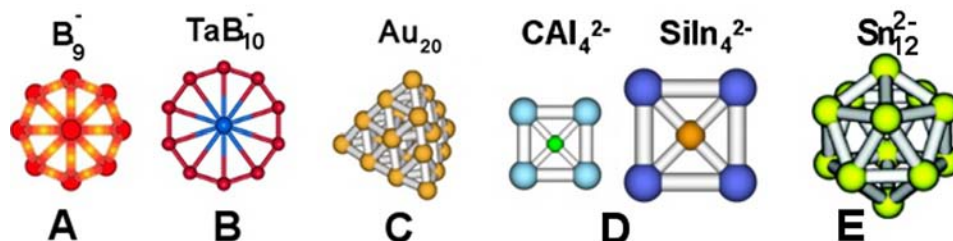


Figure 1. Representatives of unusual clusters: A) B_9^- is a wheel (Zhai et al. 2003). B) TaB_{10}^- (Galeev et al. 2012). C) Au_{20} (Zubarev and Boldyrev 2009). D) Clusters containing tetracoordinated planar C and Si atoms (Alexandrova et al. 2012). E) Stannaspherene (Cui et al.).

Clusters are relatively rare in Nature, because free clusters tend to merge to form bulk materials whenever there is a chance. However, stable clusters can be secured in binding sites of proteins, or pores of materials, or decorated with protecting ligands in solution. Clusters can be obtained in the laboratory, either synthetically in solution, or in the gas phase using, for instance, laser ablation or thermal evaporation followed by mass selection. Properties of clusters can be assessed spectroscopically, providing structural and electronic signatures, in conjunction with theoretical studies. In fact, theory has become indispensable in providing a full picture of clusters' structures, bonding, and properties. One of the major reasons theory is required in studies of clusters is that

potential energy surfaces of clusters are very complex with many local minima close in energy, and the global minima of clusters can have most unexpected shapes.

Whether natural or manmade, clusters found in various contexts often exhibit remarkable properties. For example, clusters can be catalytic,(Arenz et al. 2006; Chrétien et al. 2008; Chrétien and Metiu 2006; Haruta and Date 2001; Heiz et al. 1999; Kaden et al. 2009; Lee et al. 2004; Lopez and Norskov 2002; Molina and Hammer 2005; Remediakis et al. 2005; Sanchez et al. 1999; Vajda et al. 2009; Valden et al. 1998; Yoon et al. 2005; Zhai et al. 2010) some clusters can be incorporated into materials as building blocks or ligands,(Alexandrova et al. 2005; Alexandrova et al. 2006; Alexandrova et al. 2004; Castleman and Khanna 2009; Claridge et al. 2009; Fehlnner et al. 2005; Fokwa and Hermus 2012; Guennic et al. 2004; Jadzinsky et al. 2007; Reber et al. 2007) and certain clusters can be high-temperature superconductors (de Heer 1993; Kresin 2012; Kresin and Ovchinnikov 2008, 2012). Albeit, these applications often result from exhaustive searches for suitable cluster-containing materials, without much rationale.

Our intuition breaks down when it comes to cluster shapes and properties, because we poorly understand their electronic structure. For chemists, electronic structure traditionally translates into the language of chemical bonding, i.e. a set of qualitative concepts, such as 2 center – 2 electron (2c-2e) bond, lone electron pair, conjugation and hyperconjugation, aromaticity, etc. These concepts are then helpful in the rationalization, prediction, and design of molecular or material properties. Considering the wealth of new applications possible for clusters, it is of course most desirable to have a predictive and intuitive language like this also for clusters. The language of chemical bonding in clusters

is currently undergoing an explosive development, but it is far from being complete. So far, we find that the bonding rules are more complex than in traditional molecules, and often unprecedented. Some unusual phenomena include multiple aromaticity, partial covalency even in all-metal clusters, and super-atom-like closure of molecular orbital (MO) shells. Here, we review these newly discovered principles, and the physical basis on them.

Once we understand how clusters are bound, and how, on the basis of chemical bonding, to design cluster shapes and properties at will, cluster science will become truly rational. In fact, cluster design based on chemical bonding already has successful precedents (Alexandrova et al. 2012; Galeev et al. 2012; Sergeeva and Boldyrev 2011; Tiznado et al. 2009; Zhang and Alexandrova 2013). We, as a community, are in the privileged position to write a new textbook chapter on the chemistry of clusters.

In what follows, we first discuss the main rules of chemical bonding in clusters developed to date. Then, we discuss some applications of clusters in technology, in a variety of structural contexts, to tease the reader with opportunities that clusters have in store for the future.

2. Chemical bonding phenomena in clusters

2.1. Multiple aromaticity and antiaromaticity (σ , π , δ) in 2-D and 3-D.

Aromaticity is the bonding phenomenon associated with increased symmetry, stability, and specific reactivity. First developed for organic molecules, it has been indispensable

for rationalization of their symmetric shapes and reactivity (Minkin et al. 1994). It turns out that this important concept belongs even more naturally to the chemistry of clusters.

The discovery of aromaticity in all-metal clusters is one of the most remarkable developments in cluster science (Boldyrev and Wang 2005; Kuznetsov et al. 2003; Li et al. 1995; Li et al. 2001). It is also surprising that it took so long to discover. Indeed, metallic clusters are electron-deficient, in this sense that they do not have enough valence electrons available to bind each pair of atoms via 2c-2e bonds. Therefore, as much as bonding in bulk metals is delocalized, bonding in all-metal clusters will exhibit similar delocalized behavior. Delocalized bonding is traditionally described by chemists as aromatic or antiaromatic, depending on the population of degenerate sets of MOs manifested in electron counting Hückel's rules (Minkin et al. 1994). Therefore, the presence of aromaticity and antiaromaticity in all-metal clusters is absolutely natural, and, once discovered, its importance was immediately recognized in the scientific community.

The range of atomic orbitals (AOs) (s, p, d, f, etc.), and the resultant bonding overlaps (σ , π , δ , etc.) available for bonding in inorganic clusters is wider than that in organic compounds. Hence, aromaticity and antiaromaticity also can be of more than one type. For example, small alkali clusters exhibit pure σ -aromaticity or antiaromaticity, without any involvement whatsoever of the π -MOs (Alexandrova and Boldyrev 2003). Notice that σ -overlap simply results from each two neighboring AOs interacting with each other through just one lobe. π -overlap combines two lobes, δ -overlap utilizes three lobes, etc. The most interesting situations arise, however, when more than one type of

(anti)aromaticity are present in a cluster simultaneously. For example, clusters of Al exhibit aromaticity and antiaromaticity of both π - and σ -types, and the latter is of two different kinds: radial and peripheral (Kuznetsov et al. 2003; Li et al. 2001). This is explained as follows. In one such cluster, Al_4^{2-} (Figure 2A), whose ground states was determined to be a perfect square, MOs formed by 3s- and the 3s- and 3p-AOs completely separate, i.e. no sp-mixing takes place. The deepest four valence MOs in Al_4^{2-} (labeled as 3s LP in Figure 2A) are formed by 3s-AOs, and, being completely populated

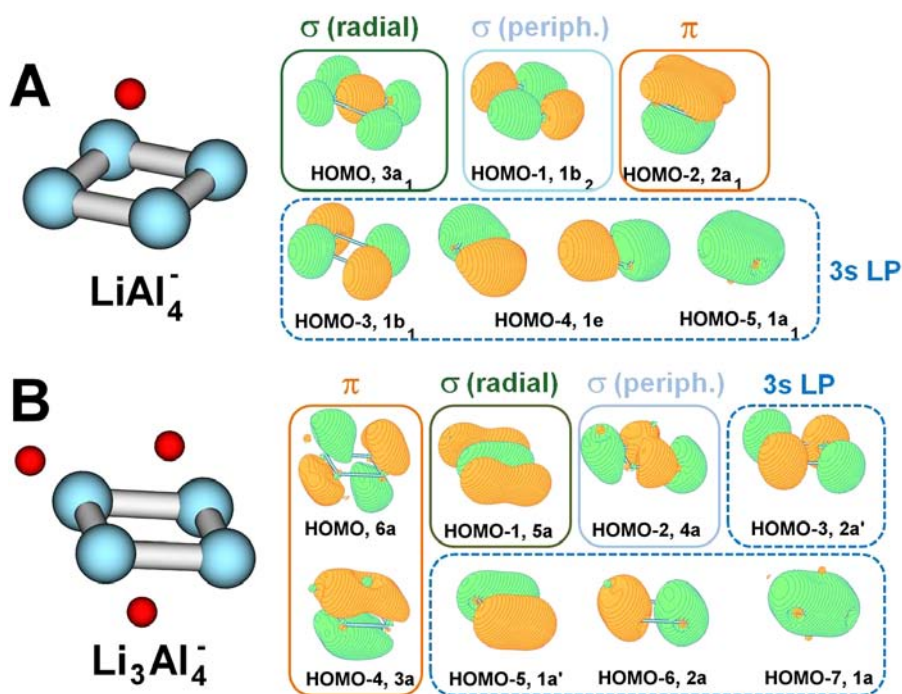


Figure 2. (A) Left: LiAl_4^- structure; right: atomic charges, and populated valence MOs of Al_4^{2-} (Li et al. 2001). (B) Left: Li_3Al_4^- structure and atomic charges; right: populated valence MOs of Al_4^{4-} (Kuznetsov et al. 2003). MO types are labeled as σ -radial, σ -peripheral, π -, or LP (lone pair), as described in the text.

by eight electrons, they contribute nothing to the overall bonding of the cluster. They can be viewed as 3s-lone pairs on Al atoms. The remaining three populated valence MOs originate from three sets of orthogonal 3p-AOs on atoms. The HOMO of the cluster is a completely bonding π -MO formed by the AOs overlapping above and below the cluster plane. This MO makes the species obey the $(4n+2)$ Hückel's rule for aromatic compounds with $n=0$, and the cluster is π -aromatic. The HOMO-1 is formed by 3p-AOs that lay in the cluster plane and overlap in the center of the square. This MO is responsible for the σ -aromaticity in the system. Finally, the HOMO-2 is another completely bonding fully delocalized σ -MO formed by the last set of 3s-AOs. The HOMO-2 gives the cluster the second type of σ -aromaticity. Hence, the cluster is triply-aromatic. This bonding situation is unheard of in the prototypical organic world, where aromaticity never goes beyond the π -type.

Making the cluster antiaromatic in at least one of the subsystems of MOs leads to a geometric distortion. For example, Al_4^{4-} stabilized by alkali metal cations (Figure 2B) is an example of an all-metal π -antiaromatic system. In this case, the extra two electrons in the Al-core (as compared to Al_4^{2-}) go to the nonbonding π -MO possessing a single nodal plane. Its counterpart with the nodal plane perpendicular to the one in the HOMO is unoccupied. The partial population of the formerly degenerate delocalized MOs is a signature of antiaromatic compounds. Indeed, Al_4^{4-} has four π -electrons, obeying the $4n$ Hückel's rule for antiaromatic compounds, with $n=1$. As a result, the cluster undergoes a first order Jan-Teller distortion toward a rectangular shape. The two σ -subsystems of

MOs remain the same as in Al_4^{2-} , and so Al_4^{4-} is doubly- σ -aromatic. This is a case of so-called “conflicting aromaticity”.

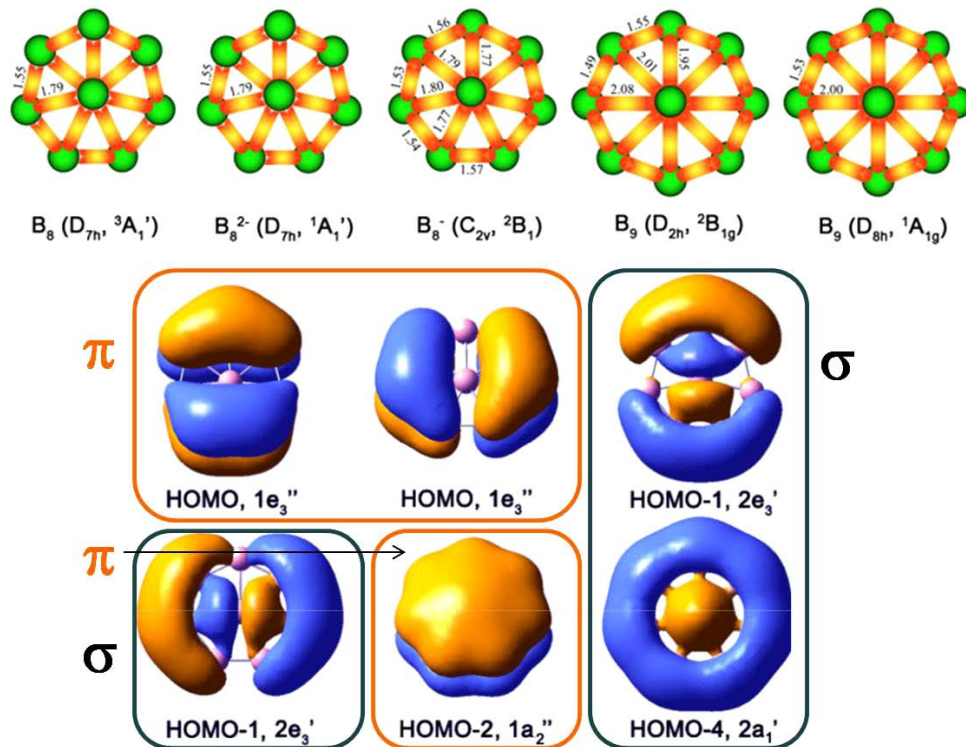


Figure 3. Boron wheels, and their delocalized valence MOs responsible for the doubly-aromatic character of chemical bonding (Zhai et al. 2003).

A remarkable showcase of double aromaticity and its impact on cluster shapes can be found in B_8 and B_9 clusters of boron with different charges (Zhai et al. 2003). In Figure 3, we show only completely delocalized valence MOs in these clusters. Three of them (HOMO, and HOMO-2) are the π -type MOs; they resemble the π -MOs of benzene. The six electrons populating these MOs make the cluster π -aromatic, in accord with the $(4n+2)$ Hückel’s rule. In addition, the delocalized subsystem of σ -MOs exhibits the

analogous population by six electrons, rendering the clusters also σ -aromatic. Beautiful symmetric shapes result from this double aromaticity (Figure 3). Additionally, also driven by double aromaticity, the central B atoms exhibit extreme coordination numbers of 7 and 8, which are unprecedented for the chemistry of boron. Since 2003, a record for coordination number in plane of 10 was made in TaB_{10}^- (Figure 1B), with the Ta atom residing in the center of the flat B_{10} cycle (Galeev et al. 2012). TaB_{10}^- is also doubly-aromatic.

Taking the story further, some clusters exhibit δ -aromaticity, i.e. a delocalized δ -type overlap characterized by the partial population of the resultant delocalized MOs that does not break the symmetry. δ -bonding is only possible in inorganic clusters formed by transition metals or lanthanides and actinides. Ta_3O_3^- was the first cluster where δ -aromaticity due to the presence of two δ -electrons was observed (Figure 4) (Zhai et al. 2007). The HOMO-1 is the δ -type MO. Notice that the cluster also exhibits π -aromaticity (two π -electrons populating the HOMO-2), and σ -aromaticity (six σ -electrons populating the doubly-degenerate HOMO and the HOMO-3). The cluster is triply-aromatic. The perfect triangular shape is explained by the stabilizing and symmetrizing effects of aromaticity.

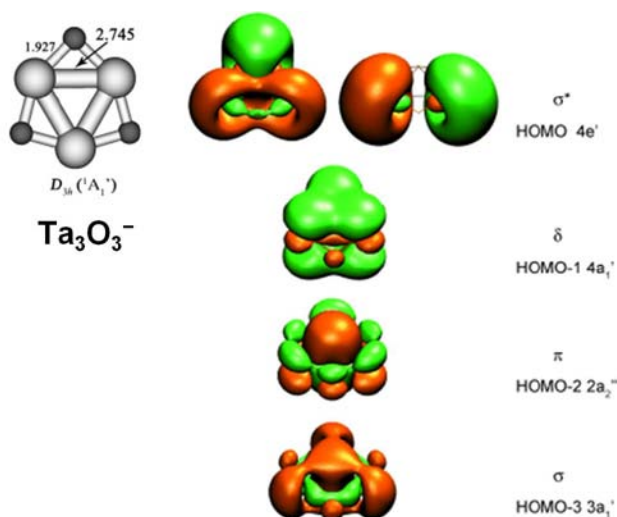


Figure 4. (A) Ta_3O_3^- the first cluster possesses π - and δ -aromaticity (Zhai et al. 2007). Reprinted with permission from Zhai H-J, Averkiev BB, Zubarev DY, Wang L-S and Boldyrev AI (2007). " δ Aromaticity in $[\text{Ta}_3\text{O}_3]^-$." *Angew. Chem. Int. Ed.* **46**: 4277-4280.

3-D aromaticity. The concept of aromaticity was originally developed for 2-D molecules of special symmetry and stability. However, aromaticity and antiaromaticity are just descriptors of delocalized bonding, stabilizing and destabilizing, respectively, and it is now realized that they do not have to be restricted to two dimensions. 3-D aromaticity is characteristic of small clusters of globular shapes, and represents a close analog of metallic bonding at the cluster scale, subject to quantum confinement. For example, clusters of Au (Figure 5) exhibit 3-D aromaticity (Zubarev and Boldyrev 2009). If one applies an electron localization analysis (AdNDP in this case (Zubarev and Boldyrev 2008)), it would be observed that the maximal localization corresponds to two

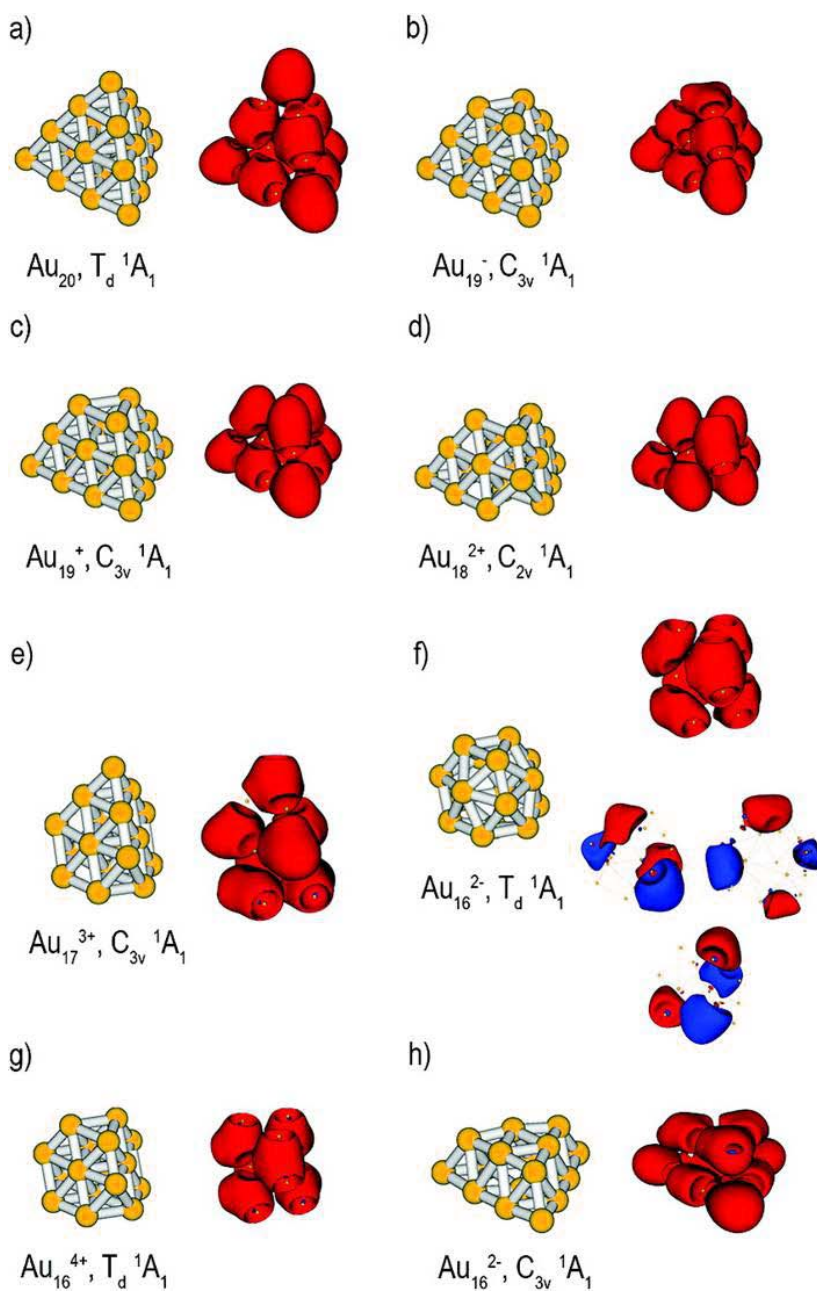


Figure 5. Structures of the gold clusters derived from the tetrahedral Au_{20} species and patterns of chemical bonding according to AdNDP (Zubarev and Boldyrev 2009).

Reprinted with permission from Zubarev DY and Boldyrev AI (2009). "Deciphering Chemical Bonding in Golden Cages." *J. Phys. Chem. A.* **113**: 866-868.

electrons being shared by an elementary tetrahedral unit, Au_4 , in the structure of each cluster. Similar phenomena can be observed in clusters of alkali metals, as small as Li_4^{2+} , which is a tetrahedral cluster with just one delocalized σ -MO in 3-D (Alexandrova and Boldyrev 2003). Hückel's electron counting rules also apply to 3-D aromaticity, and in fact they constitute an alternative way to the "super-atom" concept described below for the description of such bonding. As a matter of fact, aromaticity comes down to systems having complete or exactly half populations of degenerate sets of MOs while having an insufficient number of electrons to be localizable as 2c-2e bonds or lone pairs. Hückel's rule, super-atom concept, etc. are no more than qualitative, back of the envelope models developed to help chemists understand and rationalize these scenarios. These rules are grounded in rigorous, first-principle, quantum mechanical calculations.

2.2. Covalency in clusters and its conflict with aromaticity. In some clusters, e.g. clusters of B, Si, and even metals (Alexandrova 2012; Alexandrova et al. 2006; Alexandrova et al. 2011; Alexandrova et al. 2012; Zhai et al. 2004; Zubarev et al. 2006), aromaticity and covalency are observed simultaneously. Covalency is especially surprising when observed in all-metal clusters, because metallic systems in the bulk are usually not suspected in having covalent bonding. Furthermore, as we will show now, covalency and aromaticity work in opposite ways when defining cluster structures (Alexandrova et al. 2011; Alexandrova et al. 2012; Huynh and Alexandrova 2011).

Let us introduce the idea again using the clusters of boron, which, in addition to (anti)aromaticity, exhibit covalent bonding (Alexandrova et al. 2006). In B, the 2s-2p-AO

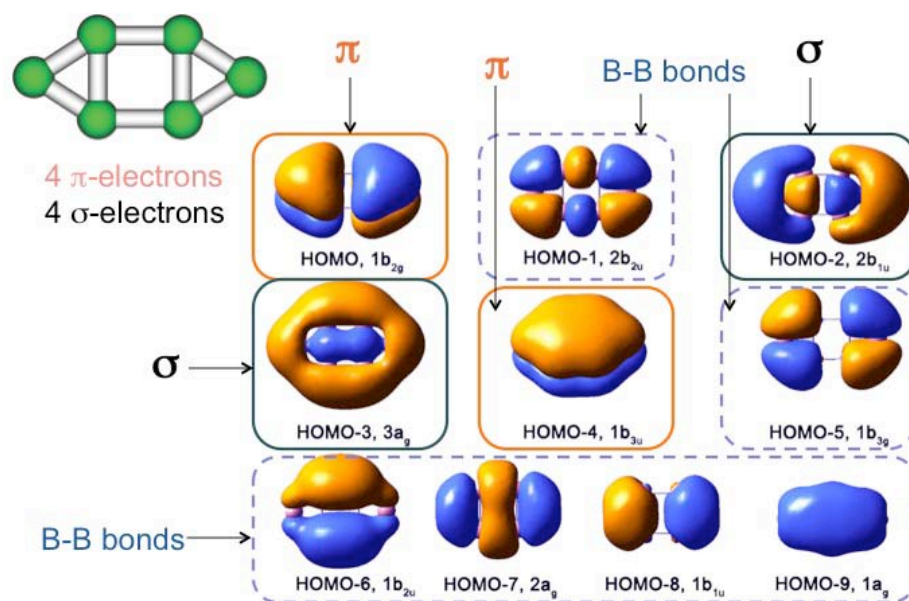


Figure 6. B_6^{2-} and its valence MOs. The decomposition of the MOs onto those of π - and σ -type, and localizable as 2c-2e B-B bonds is shown (Alexandrova et al. 2003).

energy separation is small, and these AOs can hybridize. Hybridization is generally acquired to create a better covalent overlap. Indeed, all boron clusters acquire a set of covalent 2c-2e B-B bonds. Consider the B_6^{2-} cluster shown in Figure 6 (Alexandrova et al. 2003). We can immediately detect double antiaromaticity: the HOMO and HOMO-4 make the cluster π -antiaromatic, and the HOMO-2 and HOMO-3 make the cluster σ -antiaromatic. Double antiaromaticity is responsible for the distortion of the system away from a perfect hexagon. The HOMO-1, HOMO-5, HOMO-6, HOMO-7, HOMO-8, and HOMO-9 in this cluster constitute a new bonding element. They can be localized as 2c-2e B-B bonds along the periphery of the distorted hexagon. 2c-2e B-B bonds are also found along the periphery of the boron wheels shown in Figure 3. Covalent bonding leads

to flat wheel and raft-like shapes in all small boron clusters, which is very unusual for the chemistry of boron that tends to be full of cage-like boranes and carboranes. The two types of (anti)aromaticity then render the flat structures more or less symmetric (Alexandrova et al. 2006; Martínez-Guajardo et al. 2011; Piazza et al. 2012; Sergeeva et al. 2011; Zhang et al. 2012).

In order to see how covalency opposes aromaticity in defining cluster shapes, and how it flattens B clusters, consider the following paradox: B and Al are elements located one just above the other in the periodic table and having the same number of valence electrons, 3. However, the clusters B_6^{2-} and Al_6^{2-} (as doubly-charged anions, or as salts neutralized by Li or Na cations), for example, have distinctly different shapes (Figure 7). B_6^{2-} is flat (Alexandrova et al. 2003), whereas Al_6^{2-} is octahedral (Kuznetsov et al. 2002). The reason for this is that B is capable of covalent bonding, whereas Al is not (Huynh and Alexandrova 2011). The 2s- and 2p-AOs in B can form $s^n p^m$ -hybrids, whereas the 3s- and 3p-AOs in Al are far enough apart in energy to prevent mixing. So the 2c-2e bonds are possible in B clusters, but impossible in Al clusters. The entire bonding in Al clusters thus comes from the delocalized overlap in the 3p-subspace. Delocalized overlap is obviously stronger when the system is compact. Hence, the octahedral shape of Al_6^{2-} . Notice that in flat B_6^{2-} the quality of the delocalized bonding is necessarily compromised: the overlap is smaller in 2-D, and the antiaromaticity that results from it is an antibonding effect. B_6^{2-} sustains the weaker delocalized overlap in order to attain covalent bonding instead! Thus, covalency drives the cluster toward 2-D, whereas aromaticity drives it toward 3-D.

Figure 7. B_6^{2-} and Al_6^{2-} have different structures rooted in the differences in chemical bonding (Alexandrova et al. 2003; Huynh and Alexandrova 2011; Kuznetsov et al. 2002). The B cluster has covalent bonding that defines its planar shape, whereas in the Al cluster all bonding is delocalized. Reprinted with permission from Huynh MT and Alexandrova AN (2011). "Persistent Covalency and Planarity in the $B_nAl_{6-n}^{2-}$ and $LiB_nAl_{6-n}^-$ ($n=1-6$) Cluster Ions." *J. Phys. Chem. Lett.* **2**: 2046-2051.

To demonstrate the idea further, aromaticity and covalency can be deliberately set in conflict in the series, $B_nAl_{6-n}^{2-}$. Indeed, as the Al content grows, the onset of 3-D structures takes place. Furthermore, this onset is late in the series, which is a manifestation of covalency being a more dominant bonding effect. The mid-point in the series, $B_3Al_3^{2-}$ is still flat with a B_3 -triangle located in the center of the cluster surrounded by the Al atoms (Huynh and Alexandrova 2011).

Another example of covalency and aromaticity opposing each other is the doped clusters of alkali metals, LiNa_4^- and LiK_4^- , shown in Figure 8 (Alexandrova 2012). It is surprising that these two clusters are bound and shaped differently, since we usually believe in valence-isoelectronic substitution in chemistry. Due to the complementarity of AO-sizes and energies of Li and Na, Li undergoes the 2s-2p-hybridization, and then binds to the Na portion of the cluster in a more directional and partially covalent manner. The cluster undergoes a second order Jahn-Teller distortion toward a C_{2v} shape (Figure 8). In contrast, AOs of Li and K are significantly different in energy and size, and their overlap cannot be made efficient, whether or not hybridization takes place. Therefore, when the K cluster is doped with Li, Li does not hybridize but instead uptakes an extra electron, leaving the K_4 -core close to charge-neutral. The K_4 -core then exhibits σ -aromaticity: the three valence σ -MOs are populated by six electrons. Aromaticity then drives the cluster toward a symmetric D_{4h} shape. Covalency, on the other hand, is destructive to symmetry.

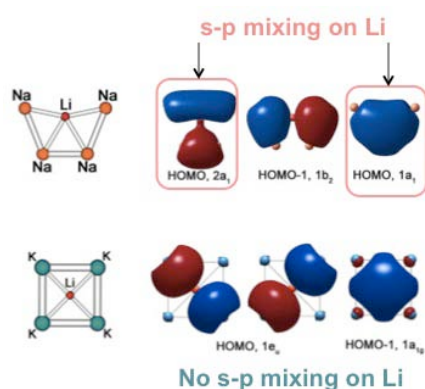


Figure 8. LiNa_4^- versus LiK_4^- : their different global minimum structures and valence

MOs. The s-p hybridization of AOs on Li in one case but not in the other is illustrated (Alexandrova 2012).

Clusters of Al, Ga, and In doped with C, Si, and Ge are another example of aromaticity and covalency being in contradiction in governing cluster shapes (Alexandrova et al. 2012). Clusters in this series also exhibit a structural trend between planar C_{2v} and square D_{4h} , correlating with partial covalency and aromaticity, respectively (Figure 9) (Alexandrova et al. 2012; Boldyrev et al. 2000; Li et al. 2000). A counterintuitive observation can be made for the doped Al clusters: in the CAl_4^- , $SiAl_4^-$, and $GeAl_4^-$ series, the strongest sp-hybridization is found in Ge, it is weaker in Si, and it is zero in C. Usually, we think that AOs have a greater tendency to hybridize when they are closer in energy, and, since the 2s-2p energy separation in C is smaller than the 3s-3p and 4s-4p separation in heavier Si and Ge, we suspect C in hybridizing more easily. Hybridization of AOs in C defines all of organic chemistry, indeed. However, in the examined clusters series, the trend is the opposite! This is again due to the quality of the overlap between the AOs of the dopant and those of the Al-core of the cluster. Because Si and Ge can achieve a more efficient overlap with Al, they undergo hybridization, whereas lighter C does not. Using this understanding of the attainability of covalency, one can predict how other clusters formed by groups III and IV would be shaped. CAl_4^- and $SiIn_4^-$ are square and aromatic, whereas $SiAl_4^-$, $GeAl_4^-$, $SiGa_4^-$ are distorted and exhibit partial covalency (Alexandrova et al. 2012). Hence, covalency is driven by the

energy-proximity of the hybridizing AOs, and by the quality of the covalent overlap that can be achieved through this hybridization.

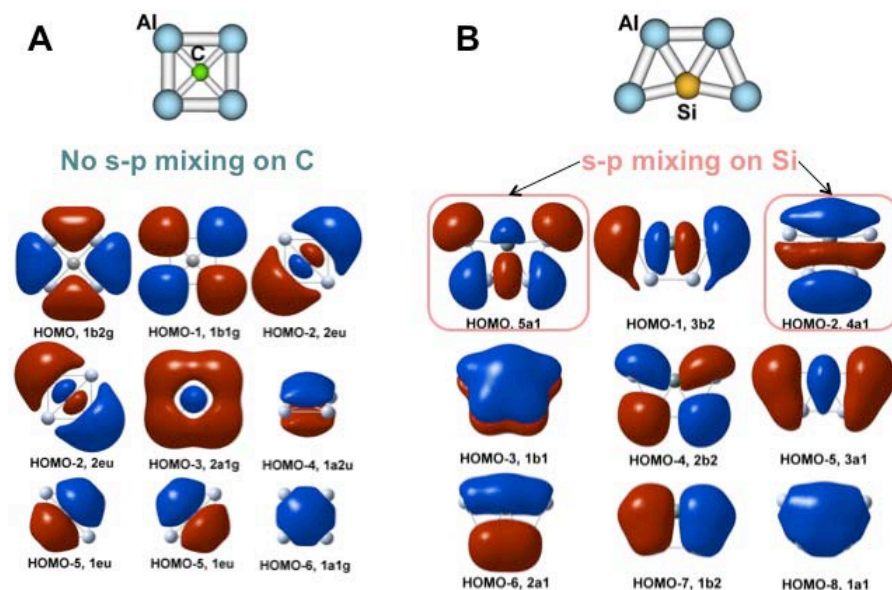


Figure 9. (A) CAI_4^- , (B) $SiAl_4^-$ as a representative of all tetraatomic C_{2v} clusters of the group III doped with a single group IV atom. The AO hybridization is demonstrated in (A), as opposed to (B). Square clusters are CAI_4^- and $SiIn_4^-$. Distorted covalent clusters are $SiAl_4^-$, $GeAl_4^-$, $SiGa_4^-$ (Alexandrova et al. 2012).

To summarize, what has been observed in a number of examples is how covalency in general is associated with the reduction of cluster symmetry, whereas aromaticity drives them toward more symmetric shapes. Covalency and aromaticity are therefore two tuning knobs of cluster design.

2.3. Ionic bonding and its support for stabilizing bonding effects. Partially ionic bonding takes place when atoms of substantially different electronegativities bind, as is well-known. However, the degree of ionicity (i.e. intra-cluster charge transfer) varies not

only due to the differences in electronegativities of the constituting elements, but also due to the bonding character that can be attained through this charge transfer, as will be demonstrated shortly. Although this effect is rather subtle, it is definitely present, and in some cases may manifest itself in unique ways.

Consider the binary cluster ions, LiAl_4^- and Li_3Al_4^- . As explained above, Al_4^{2-} is a triply-aromatic cluster (Li et al. 2001), and Al_4^{4+} is antiaromatic in its π -subsystem of MOs (Kuznetsov et al. 2003). The bare Al_4 ions would be unstable against electron ejection in vacuum, so they are stabilized by coordination to Li^+ to partially compensate the negative charge. The bonding between Li and Al parts is only partially ionic, since the electronegativities of Li and Al are not that different (0.98 and 1.61, respectively). Notice, however, when Li binds ionically to Al_4^{2-} , it sustains the triply-aromatic character of the anion, whereas when Li binds ionically to Al_4^{4+} , it contributes to its π -antiaromatic character (since the HOMO is the formerly doubly-degenerate π -MO). In other words, charge transfer to Al_4^{2-} would mean stabilization, whereas charge transfer to Al_4^{4+} would mean destabilization of the Al core. Quite naturally then, the charge transfer from the three Li atoms to Al_4 is more pronounced in LiAl_4^- than in Li_3Al_4^- . Calculations show that the charge on Li is +0.343e in LiAl_4^- , while the average charge on the Li cations in Li_3Al_4^- is +0.326e. The effect is subtle but present.

Now consider the anionic doubly-aromatic and doubly-antiaromatic clusters of B, B_8^{2-} and B_6^{2-} (Alexandrova et al. 2005; Alexandrova et al. 2004). Both can be stabilized by Li cations, and Li coordination does not perturb the bonding or shape of these clusters (Figure 10). The overall charge transfer in LiB clusters is greater than in LiAl clusters,

because the electronegativity of B is 2.04, i.e. 1.06 units greater than that of Li. However, the charge transfer from Li to B_6^{2-} supports the destabilizing antiaromatic character of chemical bonding in this system, whereas the charge transfer from Li to B_8^{2-} supports its stabilizing doubly-aromatic character of chemical bonding. Based on this, one would expect greater charge transfer in the latter case. This is indeed true: $Q(\text{Li}) = +0.710e$ in LiB_6^- , and $Q(\text{Li}) = +0.916e$ in LiB_8^- (now a significant difference). Again, it is the nature of the chemical bonding attained in the species by virtue of charge transfer that alters the degree of charge transfer.

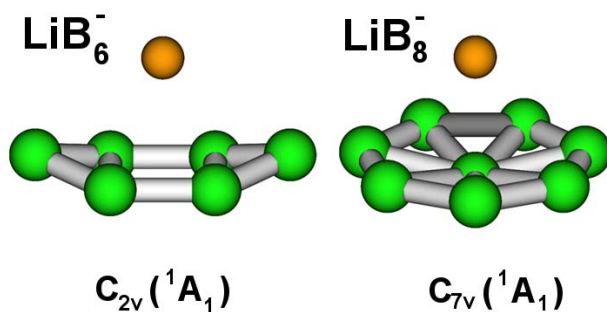


Figure 10. LiB_6^- and LiB_8^- , the prototypic clusters containing doubly-antiaromatic and doubly-aromatic all-boron ligands (Alexandrova et al. 2005; Alexandrova et al. 2004).

There are even more extreme cases of ionicity as a supporting effect for aromaticity. $\text{Li}_6\text{B}_6\text{H}_6$ contains the highly-charged core, $\text{B}_6\text{H}_6^{6-}$, with the NPA charge close to -6 (Alexandrova et al. 2003; Alexandrova and Boldyrev 2004). The transfer of six electrons to the borane core makes $\text{B}_6\text{H}_6^{6-}$ isoelectronic to benzene, C_6H_6 . The system is π -aromatic and has the same flat hexagonal shape as benzene. This extreme charge

transfer is driven by the stabilizing effect of aromaticity in $\text{Li}_6\text{B}_6\text{H}_6$ and in other highly-charged borane analogs of aromatic hydrocarbons.

The doped alkali clusters mentioned above represent a subtler example, where electronegativities do not differ substantially. All constituent elements are metals. However, in LiK_4^- , aromaticity is attained together with partial charge transfer to the dopant atom. In LiNa_4^- , covalency is adopted instead, and aromaticity and ionic bonding are abolished (Alexandrova 2012). $Q(\text{Li}) = -1.12e$ in LiK_4^- , and $Q(\text{Li}) = -0.81e$ in LiNa_4^- .

What is being observed so far is that all the usual phenomena, such as aromaticity, covalency, and ionic bonding are attainable in clusters simultaneously. However, all of them exhibit larger diversity and flexibility than in the prototypic world of organic compounds. Also, the interplay between the three phenomena is intriguing, where some of the effects can go together, and some can be orthogonal. Covalency opposes aromaticity, and the degree of ionicity depends not only on the differences in electronegativities, but also on whether or not charge transfer can enhance other stabilizing effects in the cluster, such as aromaticity, or discourage destabilizing effects, such as antiaromaticity.

2.4. Super-atom model is a specific way of viewing and rationalizing clusters that deserves special attention due to its popularity and attractiveness. It is attractive in its simplicity, though also rather restricted in the class of clusters to which it can be straightforwardly applied (Kuznetsov et al. 2002). The idea is that MOs in clusters can be viewed as analogs of AOs in atoms, and clusters themselves can be viewed as mimics of elements in the periodic table in their chemical behavior (Bergeron et al. 2005; Castleman

and Khanna 2009; Clayborne et al. 2011; Khanna and Jena 1992, 1995; Zhang et al. 2013). History began with the milestone discovery of a shell structure in the electronic spectra of small nanoclusters of monovalent alkali atoms such as Na and K ($\sim 10^2$ or fewer delocalized electrons) by Walter Knight and co-workers (Knight et al. 1984). This was later followed by observations of shell structures in Al, Ga, In, Zn and Cd clusters (Katakuse et al. 1986; Lermé et al. 1999; Poudel et al. 2008; Ruppel and Rademann 1992; Schriver et al. 1990) as well as cluster ions of Cu, Ag and Au (Katakuse et al. 1986).

With certain aggregates of atoms, the resulting cluster can exhibit atom-like properties which are determined by the number of valence electrons. In particular, metallic clusters are characterized by the presence of delocalized electrons. The properties of the metal cluster will be determined by the valence electrons contributed to the cluster's shells by each constituent atom. For example, Ga has 3 valence electrons; a cluster of 100 Ga atoms has $3 \times 100 = 300$ valence electrons. The energy levels are generally labeled with an angular momentum quantum number ($L = s, p, d, f, \dots$), its projection m_L and a principal quantum number n . By analogy with inert atoms, the most stable clusters are those for which the energy shells are completely occupied. Such clusters are called "magic" clusters. Closed-shell configurations have 8, 20, 40, 58, 92, 132 or 138 valence electrons. The concept is closely related to the jellium shell model. The notion led to the so-called 3-D Periodic table made of clusters rather than atoms.

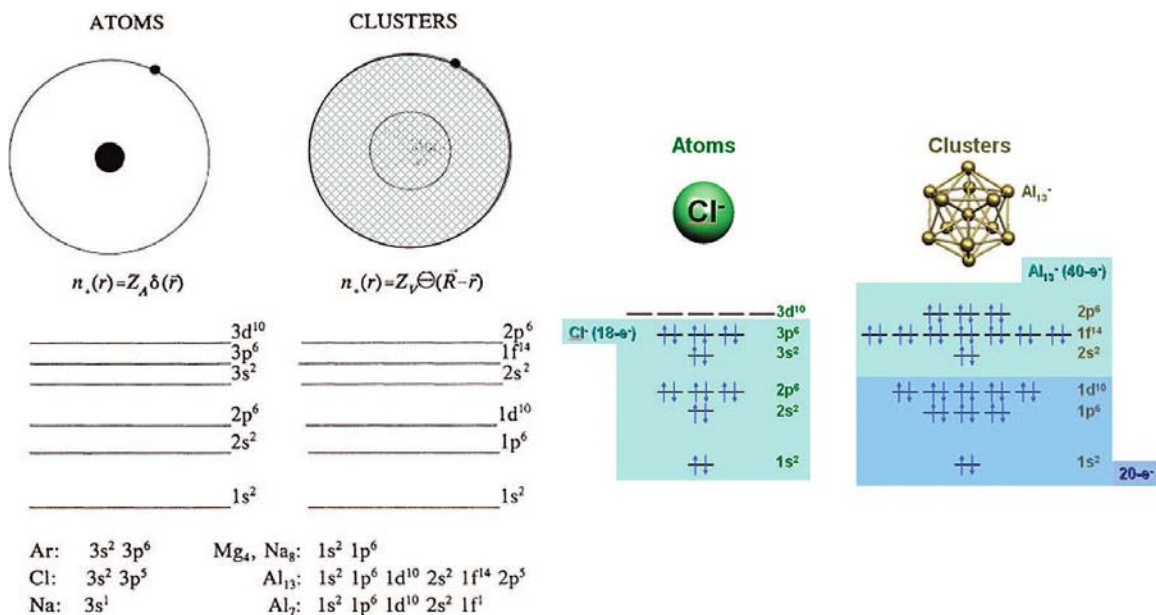


Figure 11. Energy levels in atoms and clusters. Also shown are the electronic levels in a Cl atom and that in an Al₁₃ cluster (Bergeron et al. 2005). Reprinted with permission from Castleman AW, Jr and Khanna SN (2009). "Clusters, Superatoms, and Building Blocks of New Materials." *J. Phys. Chem. C* **113**: 2664-2675.

This simple model can yield useful predictions of certain stable clusters. For example, among the clusters of Al, Al₁₃⁻ is one such “magic number” containing 40 delocalized electrons (Figure 11). Al₁₃, which has 39 valence electrons, can be stabilized either by adding one more electron to form an anion, or by replacing one Al atom with C. The Al₁₂C cluster would be energetically stable and chemically inert. The electronic structure of Al₁₂C within the jellium framework corresponds to the shell structure, 1s² 1p⁶ 1d¹⁰ 2s² 1f¹⁴ 2p⁶. The theoretical studies confirmed an increase in binding energy as an Al in Al₁₃ was replaced by C, and a corresponding decrease in reactivity (Khanna and Jena

1992, 1995). The model is indeed instrumental in predicting some cluster reactivity and even superconductivity. Reactivity-wise, for example, it was found that Al_7^- with 22 valence electrons can form stable compounds by combining with atoms that need 4 or 2 electrons to fill their shells, so that the Al_7^- cluster could close the shell of 18 or 20 electrons (Reveles et al. 2006). Also, stable super-atoms are more likely to serve as building blocks for materials.

Very recently, magnetic super-atom clusters have been reported (Zhang et al. 2013). This joint theoretical and experimental discovery indicated that the VNa_8 super-atom in particular has a magnetic moment of $5.0 \mu_B$. It is a very exciting finding, since stable species with high magnetic moments could become viable building blocks for magnetic materials.

The super-atom model is, in fact, an intuitive representation of populations of MOs applicable to metallic clusters. Simply stated, if there is no partial population of a degenerate MO in the cluster, it is going to be a “magic number”. It is best applied to metallic clusters, in which all valence MOs are delocalized over the entire cluster, and resemble most the hydrogen-like AOs. In clusters that tend to be 2-D and exhibit partially covalent bonding, this picture becomes less intuitive, although it is, of course, still correct to say that complete population of degenerate MOs leads to higher symmetry and stability.

3. Cluster-based technologies and opportunities

The understanding of chemical bonding in clusters is ultimately needed for the development of applications of clusters in materials. Such understanding must be backed by the electronic structure rationale. Opportunities for cluster material science are virtually infinite, and many of them will emerge in the years to come. Here, we will highlight just a few exciting applications, illustrating the power of understanding electronic structure of clusters for rationalization and manipulation of their properties.

3.1. New inorganic ligands and building blocks for materials. Some clusters have started making their way into inorganic and materials chemistry as new multifunctional building blocks. For example, stable super-atom clusters of Al can be incorporated in the lattice of materials (Castleman and Khanna 2009; Claridge et al. 2009; Reber et al. 2007). Furthermore, even clusters that are not classified as “magic numbers” have begun to be used in materials. For example, the doubly-antiaromatic B_6^{2-} and doubly-aromatic B_8^{2-} were successfully coordinated to metals in the gas phase without losing their structure or bonding identity (Alexandrova et al. 2003; Alexandrova and Boldyrev 2004). The flat B_6 hexagon was incorporated into a solid, $Ti_7Rh_4Ir_2B_6$ (Figure 12A) (Fokwa and Hermus 2012). Flat highly-charged boranes (Alexandrova et al. 2003; Alexandrova and Boldyrev 2004) made it into salts of transition metals, such as Re and Ru whose examples are shown in Figure 12B (Fehlner et al. 2005; Guennic et al. 2004). More composite materials of this kind are certainly underway.

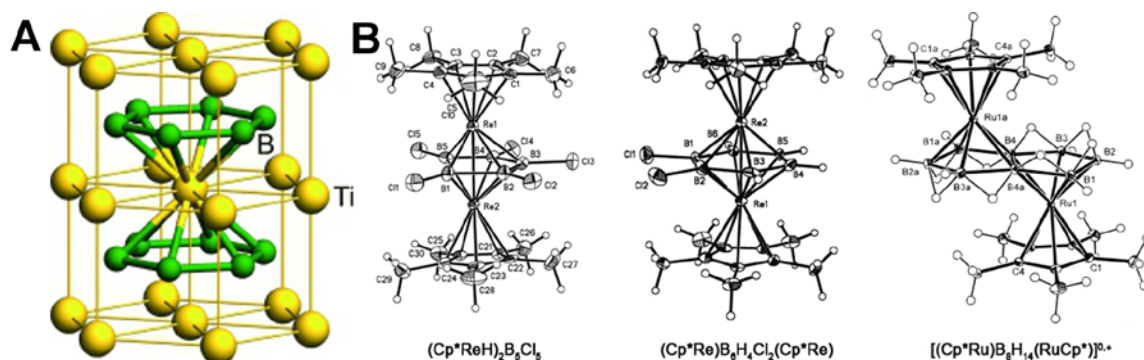


Figure 12. (A) The $\text{Ti}_7\text{Rh}_4\text{Ir}_2\text{B}_6$ solid containing the flat, highly-charged B_6 core (Fokwa and Hermus 2012). (B) Salts of Re and Ru containing flat, highly-charged boranes in the core (Fehlner et al. 2005; Guennic et al. 2004).

3.2. Superconductivity in metal clusters. This exciting application utilizes slightly larger clusters than those discussed in the previous section, however, the jellium model is suitable for their analysis. The property of superconducting property in clusters is strongly dependent on the physical size of the system (Bezryadin et al. 2000; Bose et al. 2010; Bose et al. 2005; Guo et al. 2004; Hsu et al. 2006; LeClair et al. 2005; Li et al. 2008; Li et al. 2005; Li et al. 2003; Moshchalkov et al. 1995; Reich et al. 2003). According to the Bardeen-Cooper-Schrieffer (BCS) theory, the occurrence of superconductivity is associated with the appearance of an energy gap at the Fermi energy, which corresponds to the energy needed to break up Cooper pairs. The BCS theory implicitly assumes that the size of the system exceeds the London penetration depth and the coherence length of the Cooper pairs (i.e. the size should be a few hundred nanometers). The “critical sizes” supporting superconductivity have been investigated experimentally in thin films (Ralph et al. 1997), in nanowires (Zgirski et al. 2005) and in

nanoparticles (Bose et al. 2005; Reich et al. 2003) . In small systems, superconductivity will be suppressed when the electron level separation near the Fermi energy is comparable to the BCS energy gap (Smith and Ambegaokar 1996; von Delft et al. 1996). This is known as the Anderson criterion.

If the clusters possess a shell structure (super-atoms), a special kind of superconductivity may be possible in very small nanoclusters, even if the Anderson criterion is not met (de Heer 1993; Kresin 2012; Kresin and Ovchinnikov 2008, 2012). As discussed previously, metallic clusters are characterized by the presence of delocalized electrons. The shape of magic clusters is approximately spherical and the electronic states depend on L and n . The energy levels are four-fold degenerate due to $|m_L|$ (i.e., $m_L, -m_L$) and the electron spin (i.e. $m_s = \uparrow, \downarrow$). In a conventional superconductor a common Cooper pairing mechanism involves electrons with opposite momentum and spin, i.e. $(\mathbf{k}\uparrow, -\mathbf{k}\downarrow)$ for s-wave pairing, provided that \mathbf{k} is a good quantum number. In metal nanoclusters, the momentum \mathbf{k} is not a good quantum number. Instead, the Cooper pairs are formed between electrons with opposite projections of angular momentum, i.e. $(m_L\uparrow, -m_L\downarrow)$, similar to Cooper pairing of nucleons in atomic nuclei (Bohr et al. 1958; Migdal 1959; Ring and Schuck 2004), except for the pairing mechanism which is caused by phonon-mediated electron-electron interaction in clusters (similar to that used in bulk superconductors) (Kresin and Ovchinnikov 2008). The importance of shell structure for pairing was pointed out by Friedel (Friedel 1992), who also recognized that the shell structure could lead to a high temperature superconducting state.

Because of the shell structure, the value of T_c can be very high. For example, theoretical calculations for the Ga_{56} cluster yielded $T_c \sim 145$ K, which greatly exceeds the bulk value of T_c for the same metal ($T_c \sim 1.1$ K) (Kresin 2012). In the articles (Kresin 2012; Kresin and Ovchinnikov 2008) it is shown that the most favorable values of T_c are obtained when: 1) for clusters “Fermi levels” characterized by large values of the orbital momentum, L , and 2) a relatively small energy spacing between the highest occupied and lowest unoccupied shells. In the first situation, large values of L correspond to large degeneracies [degeneracy is proportional to $(2L+1)$], which lead to a van Hove-like singularity in the density of states, driving up the value of T_c (BCS theory predicts an increase in the value of T_c with density of states at the Fermi level). Thus, to satisfy 1), large clusters are desirable, however, the requirement of a shell structure implies that clusters cannot be too large. Sizes of $\sim 10^2$ atoms appear to be most suitable (Kresin and Ovchinnikov 2008). The highest values of T_c have been predicted for certain magic clusters, and for near-magic clusters (Kresin and Ovchinnikov 2008).

Superconductivity has been observed experimentally in molecular metal-cluster compounds (Bakharev et al. 2003; Bono et al. 2007) (Ga_{84} cluster), in crystalline cluster compounds (Hagel et al. 2002), and in pure (i.e., ligand-free), size-selected, metal clusters in the gas phase (Cao et al. 2008). In the latter case, the heat capacities of Al_{45}^- and Al_{47}^- clusters were measured and T_c was found to be as high as 200 K. Smaller “magic” clusters, such as Al_{13}^- considered earlier, do not exhibit superconducting properties, because of an insufficient degeneracy of MOs at the Fermi level, as required for superconductivity.

Clusters alone cannot generate useful macroscopic superconducting currents unless they are assembled into a macroscopic structure. It has been suggested by Friedel and others that macroscopic superconductors could be created by forming a cluster crystal whereby macroscopic conduction occurs through Josephson tunneling between the clusters (Friedel 1992). A theoretical analysis of such superconducting tunneling networks can be found in (Ovchinnikov and Kresin 2012). The idea of cluster-assembled solids, whereby highly stable and symmetrical nanostructures can be realized, has been achieved in the case of C_{60} clusters. The self-assembly of C_{60} clusters leads to the formation of fullerite solid (Kratschmer et al. 1990). If the clusters are stabilized (as is the case when metal clusters are ligand-stabilized), this self-assembly approach enables new possibilities for building new materials. In these systems, there typically exists strong covalent bonding between the constituent atoms of the cluster and weaker Van der Waals interactions between the neighboring clusters.

3.3. Cluster motors. There is a single unprecedented discovery of a cluster working as a tiny photo-driven motor. Medium-size B_n clusters (B_{11}^- , B_{13}^+ , B_{19}^+ , etc.) are flat and bicyclic (Martínez-Guajardo et al. 2011; Piazza et al. 2012; Sergeeva et al. 2011). Of these clusters, B_{13}^+ is unique. It was found that the inner ring undergoes a low-barrier rotation with respect to the outer ring (Figure 13A, blue line). What is interesting about it is that the intra-cluster rotation involves minimal perturbation in the chemical bonding of the system, as expected from the small magnitude of the barrier: only delocalized σ -electron density undergoes relocation. The cluster has a small dipole moment of 0.4 Debye, and its vector rotates upon intra-cluster rotation. The rotation

occurs in the clockwise and counter-clockwise directions with equal probability, and the second law of thermodynamics is not violated.

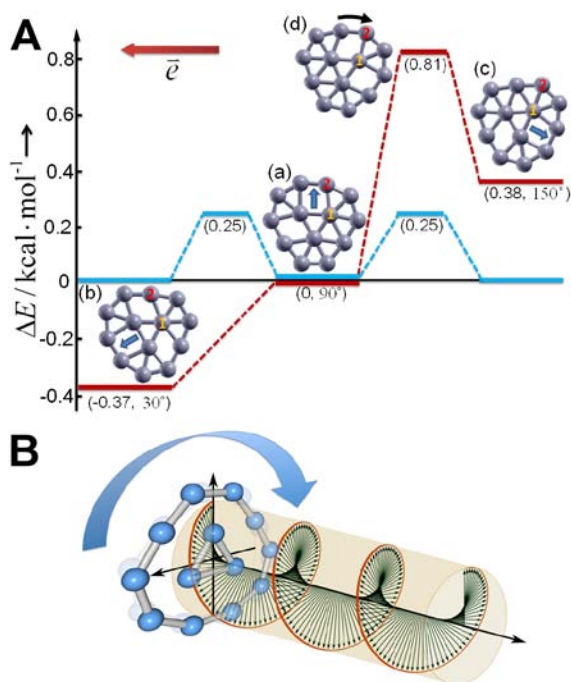


Figure 13. (A) B_{13}^+ can undergo a low-barrier intra-cluster rotation of the inner cycle with respect to the outer cycle (blue line), however, the energy landscape changes in the presence of an electric field pointing to the right: the barrier to the rotation to the left disappears, and the barrier to the rotation to the right grows 3-fold (red line). (B) Thus, in the presence of a rotating electric field in the THz range, the cluster can be driven as a wankel motor, by circularly polarized light (Zhang et al. 2012). Reprinted with permission from Zhang J, Sergeeva AP, Sparta M and Alexandrova AN (2012). "Photo-driven Molecular Wankel Engine B_{13}^+ ." *Angew. Chem. Int. Ed.* **51**: 8512-8515.

Notice now that the σ -electron density can be pulled around the cluster using circularly polarized light. In this case, the ground state Hamiltonian involves the applied electric field, and the ground state solution should exhibit a broken symmetry with respect to the direction of the intra-cluster rotation (Zhang et al. 2012). Indeed, as shown in Figure 13A (red line), the potential energy surface for the rotation is distorted in the presence of the electric field pointing perpendicular to the dipole moment: the barrier to the rotation to the left is eliminated, and the barrier to the rotation to the right grows roughly by the factor of 3. The Born-Oppenheimer molecular dynamics simulations done in the presence of a rotating electric field of 3THz indeed confirms the existence of the photo-driven cluster motor. The rotation is now unidirectional (Figure 13B). Photo-driven molecular motors are not unusual. However, what makes B_{13}^+ so distinct is that it is the first cluster motor, and it does not involve electronic excitations and internal conversion through a conical intersection back to the original geometry, but instead it is driven purely on the ground state (i.e. with minima energy dissipation).

The hope is that materials could be found where such clusters could be incorporated without the loss of their motor properties. For example, surface-deposition without binding too strongly to the surface could be a means. Also, the discovered mechanism of driving the motor by dragging non-uniformly distributed delocalized electron density could be attainable in other cluster systems. This phenomenon opens the door to the design of highly efficient engines that harness energy from electromagnetic radiation by converting it into mechanical or electrical work.

3.4. Clusters in catalysis. Clusters are natural suspects for having catalytic properties. This is well-recognized, as can be seen even just from the publications on catalytic properties of clusters toward the reaction of CO oxidation (Arenz et al. 2007; Arenz et al. 2006; Chrétien et al. 2008; Chrétien and Metiu 2006, 2008; Haruta and Date 2001; Heiz et al. 1999; Kaden et al. 2009; Landman et al. 2007; Lee et al. 2004; Lopez and Norskov 2002; Molina and Hammer 2005; Remediakis et al. 2005; Sanchez et al. 1999; Tang and Henkelman 2009; Valden et al. 1998; Yoon et al. 2005; Yoon et al. 2012; Zhai et al. 2010; Zhang and Alexandrova 2013). Indeed, many corner and edge sites and the availability of dangling orbitals for potential substrate binding, high strain for higher reactivity, and tunability of the electronic structure of clusters via their size, composition, and the environment all point at their potential to be good catalysts.

While catalysis now has a history of “going nano”, the sub-nano regime only recently picked up momentum. In order to harvest the catalytic properties of small clusters of specific sizes, clusters have to be immobilized and secured, for example on supporting surfaces, in the pores of zeolites or metal-organic frameworks, or in pockets of polymers and biomolecules. Here, we focus on surface-deposited clusters as a prominent case. As an inspirational example, Zhai et al. (Zhai et al. 2010) studied clusters of Pt of a variety of sizes deposited on silica. This system exhibits interesting catalytic activity toward the water-gas shift reaction. Intriguingly, when the system is chemically treated to undergo a shift in cluster size distribution toward smaller clusters, the catalytic activity sky-rockets. This indicates that catalysis is primarily due to the smaller clusters in

the system. The smallest size is also where clusters exhibit the most unusual and tunable chemical bonding phenomena, as articulated above.

Anderson et al. (Kaden et al. 2009; Lee et al. 2004) address the electronic structure – catalytic property dependences explicitly. They prepared size-selected clusters of Pd and Au deposited on $\text{TiO}_2(110)$, and measured their catalytic activity toward the reaction of CO oxidation as a function of cluster size (Figure 14). The dependencies were found to be highly nonlinear, and not extrapolatable to larger nanoparticles. In addition, the dependencies of catalytic activity for Pd_n and Au_n are different and almost anti-correlated. For example, there is an activity rise going from Pd_1 to Pd_2 , but a dip going from Au_1 to Au_2 , a dip at Pd_4 and Pd_5 , but a rise at Au_3 and Au_4 , etc. The erratic character of dependence for Pd_n correlates with the X-Ray photoelectron spectroscopy (XPS) shift observed for the core 3d-electrons of Pd (red line in Figure 14A), and this is a clear signal that the catalytic activity is a function of the electronic properties of the clusters. Understanding the electronic structure of deposited clusters that underlie such properties is most desirable. Catalysis on sub-nano clusters is the area where the electronic structure rationale should become the most prominent tool of the future.

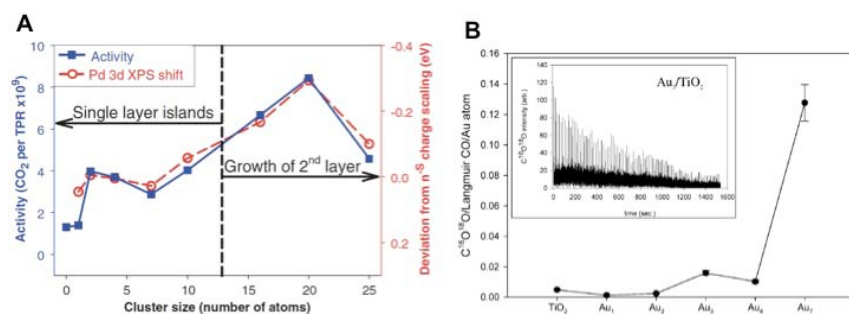


Figure 14. Catalytic activity of size-selected surface-deposited clusters as a function of cluster size. (A) Pd clusters on titania (Kaden et al. 2009), (B) Au clusters on titania (Lee et al. 2004). Reprinted with permissions from Kaden WE, Wu T, Kunkel WA and Anderson SL (2009). "Electronic Structure Controls Reactivity of Size-Selected Pd Clusters Adsorbed on TiO₂ Surfaces." *Science* **326**: 826-829; Lee S, Fan C, Wu T and Anderson SL (2004). "CO Oxidation on Au_n/TiO₂ Catalysts Produced by Size-Selected Cluster Deposition." *J. Am. Chem. Soc.* **126**: 5682-5683.

Parts of the puzzle about Au_n and Pd_n on titania have begun to emerge recently. For example, Pd, being a d¹⁰ element and having a high affinity to oxygen, preferentially binds to the stoichiometric part of the titania surface (Liu 2012; Zhang and Alexandrova 2011). It was inferred from both theory and scattering experiments that small Pd clusters lay flat on titania, i.e. they change shape from 3-D in the gas phase to 2-D upon deposition. The flat shapes are facilitated by good matching between cluster geometries and locations of protruding O atoms on the surface, and resultant covalent bonding between Pd and O (Liu 2012; Zhang and Alexandrova 2011). In addition, Pd clusters bound to titania were found to exhibit aromaticity (this was the first observation of

aromaticity in surface-deposited clusters) (Zhang and Alexandrova 2012). Specifically, Pd₄ is tetrahedral in the gas phase, but adopts a square structure when deposited on TiO₂(110). In this form the cluster exhibits double σ -aromaticity (Figure 15). Two electrons leave the manifold of MOs formed by 4d-AOs and go to the only completely bonding, fully delocalized σ -MO formed by 5s-AOs. This MO makes the cluster obey the $(4n+2)$ Hückel's rule for aromatic species with $n=0$, rendering the cluster σ -aromatic. The hole left in the set of four MOs formed by $4dx^2-y^2$ AOs makes the cluster again obey the $(4n+2)$ Hückel's rule with $n=1$, and the system is therefore doubly-aromatic. Aromaticity is associated with reduced and specific reactivity, and antiaromaticity with enhanced reactivity and lower stability. This correlation between (anti)aromaticity would be most relevant, but it remains to be demonstrated for catalytic clusters.

Au_n behave completely differently when deposited on titania and other oxides. Being more electronegative, they preferentially bind to surface O-vacancies that carry two extra electrons (Yoon et al. 2005). Au clusters are 3D on the surface. Transmitting electrons from the vacancy to the antibonding orbitals of the bound substrate (activation) is then at the heart of the catalytic mechanism. The shape of the cluster's HOMO becomes the most important electronic structure element governing cluster activity.

These stories are a beautiful beginning. We start being able to understand properties of selected surface-deposited clusters. As a dream for the near future: can we understand enough to design our clusters, and can we directly map our efforts at wave function design onto rational catalyst design?

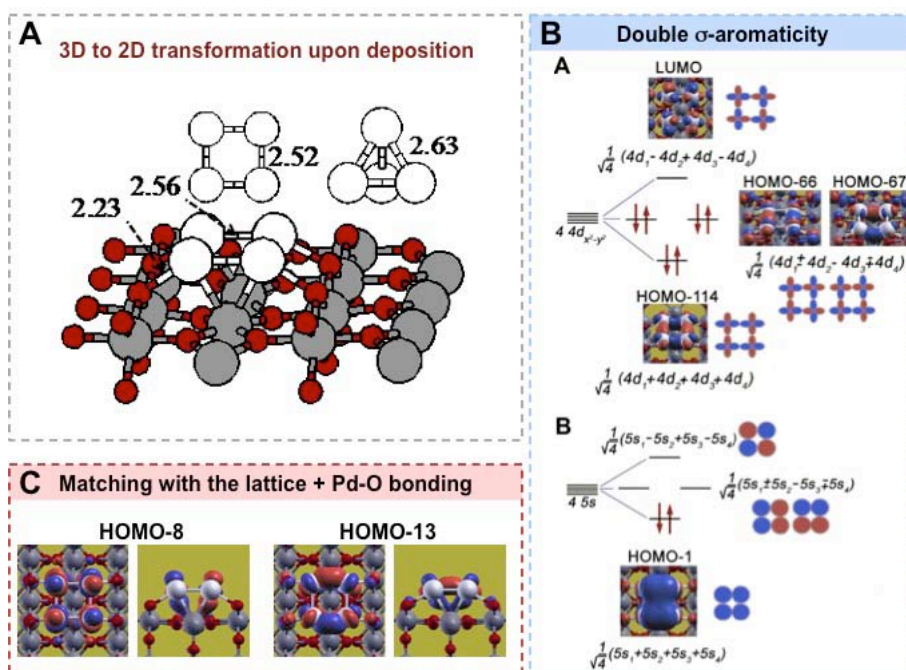


Figure 15. Chemical bonding in flat Pd₄ deposited on titania is explained: (A) Structure changes from 3D in the gas phase to 2D when the cluster is deposited on itania surface; (B) together with this, double s-aromaticity emerges in the cluster, which should correlate with specific stability and reactivity; (C) the flattening is facilitated by the matching with the surface oxygen atoms to which Pd binds (Zhang and Alexandrova 2012).

4. Conclusions

Our understanding of chemical bonding in clusters is gaining momentum, but still has a long way to go before those concepts become fully instrumental in applications of clusters to various field of technology. The bonding concepts pertaining to chemical bonding of clusters that have been realized so far include:

- i. **Multiple aromaticity and antiaromaticity.** These are most natural for metallic clusters, which are electron-deficient, i.e. do not have enough electrons to bind all atoms via 2c-2e bonds. (Anti)aromaticity can be of several different types, σ -, π -, δ -, in 2D or 3D, and all of them can be present in the same cluster at once, sometimes conflicting with each other. The wider variety of delocalized bonding phenomena stems from the wider variety of AOs available for bonding in inorganic clusters as compared to prototypical organic compounds. Aromaticity goes together with increased symmetry and stability.
- ii. **Partial covalency.** Covalency is possible even in all-metal clusters, driven by AO-hybridization, if energetically feasible. Covalency drives clusters toward less symmetric shapes, and thus opposes aromaticity. It also constitutes a stronger bonding effect than aromaticity/antiaromaticity, and can override the effect of delocalized bonding in defining cluster shapes.
- iii. **Partially ionic bonding.** Ionicity, resulting from intra-cluster charge transfer, correlates with relative electronegativities of the constituent elements. However, it can be more or less pronounced, depending on the character of chemical bonding attained in the cluster through charge transfer. Ionicity is stronger when charge transfer contributes to stabilizing bonding effects, such as aromaticity, and is weaker when charge transfer supports destabilizing effects, such as antiaromaticity.
- iv. Other new chemical bonding phenomena definitely will be discovered in the near future. So far, only limited numbers of clusters have been explored. It is likely that the most interesting new phenomena are likely to be found in clusters of f-elements,

and also doped clusters. f-elements often possess strongly correlated electron properties and large spin-orbit couplings, which would most certainly give rise to a range of interesting phenomena.

We are generally fairly versatile in interpreting cluster geometries based on the chemical bonding. We are less versatile when it comes to predicting the shapes of new clusters based on the knowledge of the chemical bonding. Furthermore, experimental observations of cluster properties found very limited interpretation from the chemical bonding perspective, and new functional cluster-based materials tend to be discovered by chance. The dependences of cluster properties (conductivity, reactivity, etc.) on the chemical bonding within clusters require extensive exploration, evolving toward being able to predict and design new functional materials. Some of the most exciting applications of small clusters include catalysis, unique composite materials, such as high-temperature superconductors, photo-driven motor systems, and more applications are waiting to be discovered. The chemical bonding rationale should be the number one tool in design of systems with specific desired properties.

Acknowledgements: This work was supported by the AFOSR 10029173-S3 grant to ANA. ANA also thanks Professor Mark Saeys for stimulating discussions and hosting her visit at the National University of Singapore, where this paper was written. L.-S. B. acknowledges useful discussions with V.Z. Kresin and V.V. Kresin and financial support from the Dreyfus (New Faculty Award) and Beckman foundations (Beckman Young Investigator Award), NSF CHE-1153159 and AFOSR/DARPA QuASAR.

References

- Alexandrova AN (2012). "Tug of war between AO-hybridization and aromaticity in dictating structures of Li-doped alkali clusters." Chem. Phys. Lett. **533**: 1-5.
- Alexandrova AN, Birch KA and Boldyrev AI (2003). "Flattening the B₆H₆²⁻ Octahedron. Ab Initio Prediction of the New Family of Planar All-Boron Aromatic Molecules." J. Am. Chem. Soc. **125**: 10786.
- Alexandrova AN and Boldyrev AI (2003). "σ-Aromaticity and σ-Antiaromaticity in Alkaline Metal and Alkaline Earth Metal Small Clusters." J. Phys. Chem. A **107**: 554.
- Alexandrova AN and Boldyrev AI (2003). "sigma-Aromaticity and sigma-Antiaromaticity in Alkaline Metal and Alkaline Earth Metal Small Clusters." J. Phys. Chem. A **107**: 554.
- Alexandrova AN and Boldyrev AI (2004). "Arachno-, Nido- and Closo-Aromatic Isomers of the Li₆B₆H₆ Molecule." Inorg. Chem. **43**: 3588.
- Alexandrova AN, Boldyrev AI, Zhai H-J and Wang L-S (2005). "Doubly-Antiaromatic All-Boron Ligand B₆²⁻ in the LiB₆⁻ molecule. Ab Initio and Photoelectron Spectroscopic Study." J. Chem. Phys. **122**: 054313.
- Alexandrova AN, Boldyrev AI, Zhai H-J, Wang L-S, Steiner E and Fowler PW (2003). "Structure and Bonding in B₆⁻ and B₆: Planarity and Antiaromaticity." J. Phys. Chem. A **107**: 1359.
- Alexandrova AN, Boldyrev AI, Zhang H-J and Wang L-S (2006). "All-boron aromatic clusters as potential new inorganic ligands and building blocks in chemistry." Coord. Chem. Rev. **250**: 2811-2866 (and references therein).
- Alexandrova AN, Boldyrev AI, Li X, Sarkas HW, Hendricks JH, Arnold ST and Bowen KH (2011). "Lithium Cluster Anions: Photoelectron Spectroscopy and Ab Initio Calculations." J. Chem. Phys. **134**: 044322.
- Alexandrova AN, Nayhouse MJ, Huynh MT, Kuo JL, Melkonian AV, Chavez GDJ, Hernando NM, Kowal MD and Liu C-P (2012). "AB₄^{2-/-} (A = C, Si, Ge; B = Al, Ga, In) Ions: A Battle between Covalency and Aromaticity, and Prediction of Square Planar Si in SiIn₄^{2-/-}." Phys. Chem. Chem. Phys. **Submitted**.
- Alexandrova AN, Zhai H-J, Wang L-S and Boldyrev AI (2004). "Molecular Wheel B₈²⁻ as a New Inorganic Ligand: Photoelectron Spectroscopy and Ab Initio Characterization of the LiB₈⁻ Anion." Inorg. Chem. **43**: 3552.
- Arenz M, Gilb S and Heiz U (2007). Atomic Clusters: From Gas Phase to Deposited. D. P. Woodruff. Oxford, Elsevier. **12 of Chemical Physics of Solid Surfaces**: 1-47.
- Arenz M, Landman U and Heiz U (2006). "CO Combustion on Supported Gold Clusters." ChemPhysChem **7**: 1871-1879.
- Bakharev ON, Zelders N, Brom HB, Schnepf A, Schnockel H and Jos de Jongh L (2003). "^{69,71}Ga NMR studies of a superconducting Ga₈₄ cluster compound." Eur. J. Phys. D **24**: 101-104.
- Bergeron DE, Roach PJ, Castleman AW, Jr., Jones NO and Khanna SN (2005). "Al cluster superatoms as halogens in polyhalides and as alkaline earths in iodide salts." Science **307**: 231-235.

- Bezryadin A, Lau CN and Tinkham M (2000). "Quantum suppression of superconductivity in ultrathin nanowires." *Nature* **404**: 971-974.
- Bohr A, Mottelson BR and Pines D (1958). "Possible analogy between the excitation spectra of nuclei and those of the superconducting metallic state." *Phys. Rev.* **110**: 936-938.
- Boldyrev AI and Wang L-S (2005). "All-Metal Aromaticity and Antiaromaticity " *Chem. Rev.* **105**: 3716-3757.
- Boldyrev AL, Li X and Wang L-S (2000). "Experimental Observation of Pentaatomic Tetracoordinate Planar Si- and Ge-containing Molecules: MA_4^- and MA_4 (M=Si, Ge)." *Angew. Chem. Int. Ed.* **39**: 3307.
- Bono D, Bakharev ON, Schnepf A, Hartig J, Schnockel H and de Jongh LJ (2007). "Magnetization studies of superconductivity in a molecular metal cluster compound." *Z. Anorg. Allg. Chem.* **633**: 2173-2177.
- Bose S, Garcia-Garcia AM, Ugeda MM, Urbina JD, Michaelis CH, Brihuega I and Kern K (2010). "Observation of shell effects in superconducting nanoparticles of Sn." *Nat. Mat.* **9**: 550-554.
- Bose S, Raychaudhuri P, Banerjee R, Vasa P and Ayyub P (2005). "Mechanism of the size dependence of the superconducting transition of nanostructured Pb. " *Phys. Rev. Lett.* **95**: 147004
- Cao B, Neal CM, Starace AK, Ovchinnikov YN, Kresin VZ and Jarrold MF (2008). "Evidence for high T_c superconducting transitions in isolated Al_{45}^- and Al_{47}^- nanoclusters." *J. Supercon. Novel Magn.* **21**: 163-166.
- Castleman AW, Jr and Khanna SN (2009). "Clusters, Superatoms, and Building Blocks of New Materials." *J. Phys. Chem. C* **113**: 2664-2675.
- Castleman AW, Jr. and Khanna SN (2009). "Clusters, Superatoms, and Building Blocks of New Materials." *J. Phys. Chem. C.* **113**: 2664-2675.
- Chrétien S, Buratto SK and Metiu H (2008). "Catalysis by very small Au clusters." *Curr. Op. Solid State Mater. Sci.* **11**: 62-75.
- Chrétien S and Metiu H (2006). "Density Functional Study of the CO Oxidation on a Doped Rutile $TiO_2(110)$: Effect of Ionic Au in Catalysis." *Catal. Lett.* **107**: 143-147.
- Chrétien S and Metiu H (2008). "O₂ evolution on a clean partially reduced rutile $TiO_2(110)$ surface and on the same surface precovered with Au_1 and Au_2 : The importance of spin conservation." *J. Chem. Phys.* **129**: 074705.
- Claridge SA, Castleman AW, Jr., Khanna SN, Murray CB, Sen A and Weiss PS (2009). "Cluster Assembled Materials." *ACS Nano* **3**: 244.
- Clayborne AP, Lopez-Acevedo O, Whetten RL, Grönbeck H and Häkkinen H (2011). "Evidence of superatom electronic shells in ligand-stabilized aluminum clusters." *J. Chem. Phys.* **135**: 094701.
- Cui L-F, Huang X, Wang L-M, Zubarev DY, Boldyrev AI, Li J and Wang L-S "Sn₁₂²⁻: Stannaspherene." *J. Am. Chem. Soc.* **128**: 8390-8391.
- de Heer WA (1993). "The physics of simple metal clusters: experimental aspects and simple models." *Rev. Mod. Phys.* **64**: 611-676.

- Fehlner TP, Ghosh S and Noll BC (2005). "Borane Mimics of Organometallic Paradigms: Synthesis and Characterization of Isoelectronic Analogs of Dinuclear Pentalene Complexes, $[(Cp^*Ru)(B_8H_{14})(RuCp^*)]^{0,+1}$." Angew. Chem. Int. Ed. **44**: 6568-6571.
- Fokwa BP and Hermus M (2012). "All-Boron Planar B6 Ring in the Solid-State Phase $Ti_7Rh_4Ir_2B_8$." Angew. Chem. Int. Ed. **51**: 1702-1705.
- Friedel J (1992). "BCS superconductivity for weakly coupled clusters." J. Phys. II France **2**: 959-970.
- Galeev TR, Romanescu C, Li W-L, Wang L-S and Boldyrev AI (2012). "Observation of the Highest Coordination Number in Planar Species: Decacoordinated $Ta@B_{10}^-$ and $Nb@B_{10}^-$ Anions." Angew. Chem. Int. Ed. **51**: 2101-2105.
- Guennic BL, Jiao H, Kahlal S, Saillard J-Y, Helet J-F, Ghosh S, Shang M, Beatty AM, Rheingold AL and Fehlner TP (2004). "Synthesis and Characterization of Hypoelectronic Rhenaboranes. Analysis of the Geometric and Electronic Structures of Species Following Neither Borane nor Metal Cluster Electron-Counting Paradigms." J. Am. Chem. Soc. **126**: 3203-3217.
- Guo Y, Zhang YF, Bao X-Y, Han T-Z and Tang Z (2004). "Superconductivity modulated by quantum size effects." Science **306**: 1915-1917.
- Hagel J, Kelemen MT, Fischer G, Pilawa B, Wisnitzer J, Dormann E, Lohneisen HV, Schnepf A, Schnockel H, Neisel U and Beck J (2002). "Superconductivity of a crystalline Ga_{84} -cluster compound." J. Low Temp. Phys. **129**: 133-142.
- Haruta M and Date M (2001). "Advances in the catalysis of Au nanoparticles." Appl. Catal. A **222**: 427-437.
- Heiz U, Sanchez A, Abbet S and Schneider W-D (1999). "Catalytic Oxidation of Carbon Monoxide on Monodispersed Platinum Clusters: Each Atom Counts." J. Am. Chem. Soc. **121**: 3214-3217.
- Hsu Y-J, Lu S-Y and Lin Y-F (2006). "Nanostructures of Sn and their enhanced, shape-dependent superconducting properties." Small **2**: 268-273
- Huynh MT and Alexandrova AN (2011). "Persistent Covalency and Planarity in the $B_nAl_{6-n}^{2-}$ and $LiB_nAl_{6-n}^-$ ($n=1-6$) Cluster Ions." J. Phys. Chem. Lett. **2**: 2046-2051.
- Jadzinsky PD, Calero G, Ackerson CJ, Bushnell DA and Kornberg RD (2007). "Structure of a thiol monolayer-protected gold nanoparticle at 1.1 Å resolution." Science **318**: 5149.
- Kaden WE, Wu T, Kunkel WA and Anderson SL (2009). "Electronic Structure Controls Reactivity of Size-Selected Pd Clusters Adsorbed on TiO_2 Surfaces." Science **326**: 826-829.
- Katakuse I, Ichihara T, Fujita Y, Matsuo T, Sakurai T and Matsuda H (1986). "Correlation between mass distributions of zinc, cadmium clusters and electronic shell structure." Int. J. Mass Spectrom. Ion Process. **69**: 109-114.
- Katakuse I, Ichihara T, Fujita Y, Matsuo T, Sakurai T and Matsuda H (1986). "Mass distributions of negative cluster ions of copper, silver, and gold." Int. J. Mass Spec. Ion Processes **74**: 33-41.

- Khanna SN and Jena P (1992). "Assembling crystals from clusters." Phys. Rev. Lett. **69**: 1664-1667.
- Khanna SN and Jena P (1995). "Atomic clusters: Building blocks for class of solids " Phys. Rev. B **51**: 13705-13716.
- Knight WD, Clemenger K, de Heer WA, Saunders WA, Chou MY and Cohen ML (1984). "Electronic shell structure and abundances of sodium clusters." Phys. Rev. Lett. **52**: 2141-2143.
- Kratschmer W, Lamb LD, Fostiropoulos K and Huffman DR (1990). "C60: a new form of carbon." Nature **347**: 354.
- Kresin V (2012). "Nanoclusters as a new family of superconductors: potential for room temperature superconductivity. ." Nov. Magn. **2**: 711-717
- Kresin VZ and Ovchinnikov YN (2008). "'Giant' strengthening of superconducting pairing in metallic nanoclusters: large enhancement of Tc and potential for room-temperature superconductivity." Physics – Uspekhi **51**: 427-435.
- Kresin VZ and Ovchinnikov YN (2012). "Superconducting state of metallic clusters: potential for room temperature superconductivity, novel nano-based tunneling networks." Nov. Magn.: DOI 10.1007/s10948-10012-11961-y.
- Kuznetsov AE, Birch KA, Boldyrev AI, Li X, Zhai H-J and Wang L-S (2003). "All-Metal Antiaromatic Molecule: Rectangular Al₄⁴⁻ in the Li₃Al₄⁻ Anion." Science **300**: 622-625.
- Kuznetsov AE, Boldyrev AI, Zhai H-J, Li X and Wang L-S (2002). "Al₆²⁻ - Fusion of Two Aromatic Al₃⁻ Units. A Combined Photoelectron Spectroscopy and Ab Initio Study of M⁺[Al₆²⁻] (M = Li, Na, K, Cu, and Au)." J. Am. Chem. Soc. **124**: 11791-11801.
- Landman U, Yoon B, Zhang C, Heiz U and Arenz M (2007). "Factors in gold nanocatalysis: oxidation of CO in the non-scalable size regime." Topics in Catal. **44**: 145-158.
- LeClair P, Moodera JS, Philip J and Heiman D (2005). "Coexistence of ferromagnetism and superconductivity in Ni/Bi bilayers." Phys. Rev. Lett. **94**: 037006
- Lee S, Fan C, Wu T and Anderson SL (2004). "CO Oxidation on Au_n/TiO₂ Catalysts Produced by Size-Selected Cluster Deposition." J. Am. Chem. Soc. **126**: 5682-5683.
- Lermé J, Dugourd P, Hudgins RR and Jarrold MF (1999). "High-resolution ion mobility measurements of indium clusters: electron spill-out in metal cluster anions and cations." Chem. Phys. Lett. **304**: 19-22.
- Li W-H, Wang C-W, Li C-Y, Hsu CK, Yang CC and Wu C-M (2008). "Coexistence of ferromagnetism and superconductivity in Sn nanoparticles." Phys. Rev. B **77**: 094508
- Li W-H, Yang CC, Tsao FC, Wu SY, Huang PJ, Chung MK and Yao YD (2005). "Enhancement of superconductivity by the small size effect in In nanoparticles." Phys. Rev. B **72**: 214516

- Li W-H, Yang CC, Tsao FG and Lee KC (2003). "Quantum size effects on the superconducting parameters of zero-dimensional Pb nanoparticles." Phys. Rev. B **68**: 184507
- Li X-W, Pennington WT and Robinson GH (1995). "Metallic System with Aromatic Character. Synthesis and Molecular Structure of $\text{Na}_2[[\text{(2,4,6-Me}_3\text{C}_6\text{H}_2)_2\text{C}_6\text{H}_3]\text{Ga}]_3$ The First Cyclogallane." J. Am. Chem. Soc. **117**: 7578-7579.
- Li X, Kuznetsov AE, Zhang HF, Boldyrev AI and Wang L-S (2001). "Observation of All-Metal Aromatic Molecules." Science **291**: 859-861.
- Li X, Zhang X-F, Wang L-S, Geske GD and Boldyrev AI (2000). "Pentaatomic Tetracoordinate Planar Carbon $[\text{CAI}_4]^{2-}$: A New Chemistry Structural Unit and Its Salt Complexes." Angew. Chem. Int. Ed. **39**: 3630.
- Liu P (2012). "Understanding the Behavior of $\text{TiO}_2(110)$ -Supported Pd_7 Cluster: A Density Functional Study." J. Phys. Chem. C **116**: 25337–25343.
- Lopez N and Norskov JK (2002). "Catalytic CO Oxidation by a Gold Nanoparticle: A Density Functional Study" J. Am. Chem. Soc. **124**: 11262-11263.
- Martnez-Guajardo G, Sergeeva AP, Boldyrev AI, Heine T, Ugalde JM and Merino G (2011). "Unravelling phenomenon of internal rotation in B_{13}^+ through chemical bonding analysis." Chem. Commun. **47**: 6242-6244.
- Migdal AB (1959). "Superfluidity and the moments of inertia of nuclei." Nucl. Phys. **13**: 655-674.
- Minkin VI, Glukhovtsev MN and Simkin BY (1994). Aromaticity and Antiaromaticity. Electronic and Structural Aspects. New York, Wiley.
- Molina LM and Hammer B (2005). "Some recent theoretical advances in the understanding of the catalytic activity of Au. ." Appl. Catal. A **291**: 21-31.
- Moshchalkov VV, Gielen L, Strunk C, Jonckheere R and Qiu X (1995). "Effect of sample topology on the critical fields of mesoscopic superconductors. ." Nature **373**: 319-322.
- Ovchinnikov YN and Kresin VZ (2012). "Cluster-based superconducting tunneling networks." Phys. Rev. B **85**: 064518
- Piazza ZA, Li W-L, Romanescu C, Sergeeva AP, Wang L-S and Boldyrev AI (2012). "A photoelectron spectroscopy and ab initio study of B_{21}^- : Negatively charged boron clusters continue to be planar at 21." J. Chem. Phys. **136**: 104310.
- Poudel B, Hao Q, Ma Y, Lan Y and Minnich A (2008). "High-Thermoelectric Performance of Nanostructured Bismuth Antimony Telluride Bulk Alloys." Science **320**: 634-638.
- Ralph DC, Black CT and Tinkham M (1997). "Gate-voltage studies of discrete electronic states in aluminum nanoparticles." Phys. Rev. Lett. **78**: 4087-4090.
- Reber AC, Khanna SN and Castleman AW, Jr. (2007). "Superatom Compounds, Clusters, and Assemblies: Ultra Alkali Motifs and Architectures." J. Am. Chem. Soc. **129**: 10189.
- Reich S, Leitus G, Popovitz-Biro R and Schechter M (2003). "Magnetization of small lead particles." Phys. Rev. Lett. **91**: 147001

- Remediakis L, Lopez N and Norskov JK (2005). "CO Oxidation on Rutile-Supported Au Nanoparticles." Angew. Chem. Int. Ed. **44**: 1824-1826.
- Reveles JU, Khanna SN, Roach PJ and Castleman AW, Jr (2006). Proc. Natl. Acad. Sci. U.S.A. **103**: 18405.
- Ring P and Schuck P (2004). The nuclear many-body problem New York, Springer.
- Ruppel M and Rademann K (1992). "Abundance distributions and ionization potentials of neutral cadmium clusters Cd_x ($x < 50$)." Chem. Phys. Lett. **197**: 280-285.
- Sanchez A, Abbet S, Heiz U, Schneider W-D, Häkkinen H, Barnett RN and Landman U (1999). "When Gold Is Not Noble: Nanoscale Gold Catalysts." J. Phys. Chem. A. **103**: 9573-9578.
- Schrivver KE, Persson JL, Honea EC and Whetten RL (1990). "Electronic shell structure of group-IIIA metal atomic clusters." Phys. Rev. Lett. **64**: 2539-2542.
- Sergeeva AP, Averkiev BB, Zhai H-J, Boldyrev AI and Wang L-S (2011). "All-boron analogues of aromatic hydrocarbons: B_{17}^- and B_{18}^- ." J. Chem. Phys. **134**: 224304.
- Sergeeva AP and Boldyrev AI (2011). "Rational Design of Small 3D Gold Clusters." J. Clust. Sci. **22**: 321-329.
- Smith RA and Ambegaokar V (1996). "Effect of level statistics on superconductivity in ultrasmall metallic grains. ." Phys. Rev. Lett. **77**: 4962-4965
- Tang W and Henkelman G (2009). "Charge redistribution in core-shell nanoparticles to promote oxygen reduction." J. Chem. Phys. **130**: 194504.
- Tiznado W, Perez-Peralta N, Islas R, Toro-Labbe A, Ugalde JM and Merino G (2009). "Designing 3-D molecular stars." J. Am. Chem. Soc. **131**: 9426-9431.
- Vajda S, Pellin MJ, Greeley JP, Marshall CL, Curtiss LA, Balentine GA, Elam JW, Catillon-Mucherie S, Redfern PC, Mehmood F and Zapol P (2009). "Subnanometer platinum clusters as highly active and selective catalysts for the oxidative dehydrogenation of propane." Nat. Mat. **8**: 213.
- Valden M, Lai X and Goodman DW (1998). "Onset of Catalytic Activity of Gold Clusters on Titania with the Appearance of Nonmetallic Properties." Science **281**: 1647-1650.
- von Delft J, Zaikin AD, Golubev DS and Tichy W (1996). "Parity-affected superconductivity in ultrasmall metallic grains." Phys. Rev. Lett. **77**: 3189-3192.
- Yoon B, Häkkinen H, Landman U, Wörz AS, Antonietti J-M, Abbet S, Judai K and Heiz U (2005). "Charging Effects on Bonding and Catalyzed Oxidation of CO on Au_8 Clusters on MgO . ." Science **307**: 403-407.
- Yoon B, Landman U, Habibpour V, Harding C, Kunz S, Heiz U, Moseler M and Walter M (2012). "Oxidation of Magnesia-Supported Pd_{30} Nanoclusters and Catalyzed CO Combustion: Size-Selected Experiments and First-Principles Theory." J. Phys. Chem. C **116**: 9594-9607.

- Zgirski M, Riikonen K-P, Touboltsev V and Arutyunov K (2005). "Size dependent breakdown of superconductivity in ultra-narrow nanowires. ." Nano Lett. **5**: 1029-1033.
- Zhai H-J, Alexandrova AN, Wang L-S and Boldyrev AI (2003). "Hepta- and Octacoordinate Boron in Molecular Wheels of Eight- and Nine-Atom Boron Clusters: Observation and Confirmation." Angew. Chem. Int. Ed. **42**: 6004.
- Zhai H-J, Averkiev BB, Zubarev DY, Wang L-S and Boldyrev AI (2007). " δ Aromaticity in [Ta₃O₃]-." Angew. Chem. Int. Ed. **46**: 4277-4280.
- Zhai H-J, Kuznetsov AE, Boldyrev AI and Wang L-S (2004). "Multiple Aromaticity and Antiaromaticity in Silicon Clusters." ChemPhysChem **5**: 1885-1891.
- Zhai Y, Pierre D, Si R, Deng W, Ferrin P, Nilekar AU, Peng G, Herron JA, Bell DC, Saltsburg H, Mavrikakis M and Flytzani-Stephanopoulos M (2010). "Alkali-Stabilized Pt-OH_x Species Catalyze Low-Temperature Water-Gas Shift Reactions " Science **329**: 1633-1636.
- Zhang J and Alexandrova AN (2011). "Structure, stability, and mobility of small Pd clusters on stoichiometric and defective TiO₂ (110) surfaces. ." J. Chem. Phys. **135**: 174702.
- Zhang J and Alexandrova AN (2012). "Double Sigma-Aromaticity in a Surface Deposited Cluster: Pd₄ on TiO₂ (110). ." J. Phys. Chem. Lett. **3**: 751-754.
- Zhang J and Alexandrova AN (2013). "The Golden Crown: How a Single Gold Atom Boosts the CO Oxidation Catalyzed by Palladium Cluster on Titania Surfaces." Submitted.
- Zhang J, Sergeeva AP, Sparta M and Alexandrova AN (2012). "Photo-driven Molecular Wankel Engine B₁₃⁺." Angew. Chem. Int. Ed. **51**: 8512-8515.
- Zhang X, Wang Y, Wang H, Lim A, Gantfoer G, Bowen KH, Jr., Reveles JU and Khanna SN (2013). "On the Existence of Designer Magnetic Superatoms." J. Am. Chem. Soc. DOI: **10.1021/ja400830z**.
- Zubarev DY, Alexandrova AN, Boldyrev AI, Cui L-F, Li X and Wang L-S (2006). "Alteration of Si₆²⁻ Structure upon Na⁺ Coordination in NaSi₆." J. Chem. Phys. **124**: 124305.
- Zubarev DY and Boldyrev AI (2008). "Developing paradigms of chemical bonding: adaptive natural density partitioning." Phys. Chem. Chem. Phys. **10**: 5207-5217.
- Zubarev DY and Boldyrev AI (2009). "Deciphering Chemical Bonding in Golden Cages." J. Phys. Chem. A. **113**: 866-868.